Interactions modales au voisinage des points exceptionnels et application pour l'atténuation acoustique

Nicolas Even, Emmanuel Perrey-Debain, Benoit Nennig, Gautier Lefebvre

16ème Congrès Français d'Acoustique
11-15 Avril 2022, Marseille

Interactions modales au voisinage des points exceptionnels et application pour l'atténuation acoustique

N. Even [a,b], E. Perrey-Debain [a], B. Nennig [b], G. Lefebvre [a]
[a] Laboratoire Roberval - UMR 7337 - CNRS - Université de technologie de Compiègne
[b] Laboratoire Quartz - EA 7393 - ISAE-Supméca,

La réalisation de traitements acoustiques dans une cavité en basses fréquences reste toujours un challenge. Les solutions classiques utilisent des matériaux poreux ou des résonateurs accordés. La plupart de ces systèmes dépendent de paramètres tels que la fréquence, l'impédance ou des paramètres liés aux matériaux absorbants. L'étude des modes acoustiques de la cavité conduit alors à la résolution de problèmes aux valeurs propres paramétriques. Dans le cas de systèmes non-conservatifs, dits non-hermitiens, certains jeux de paramètres peuvent conduire à la présence de points exceptionnels (EP). Ces derniers correspondent à des dégénérescences spectrales pour lesquelles des modes vont fusionner, que ce soient leurs pulsations et leurs déformées modales. Les modes propres ne permettent alors plus à eux seuls de décrire le comportement du système. L'objectif de cette étude est d'illustrer le rapport entre les points exceptionnel et le temps de décroissance optimal pour des modes ciblés d'une cavité. Ces effets sont illustrés numériquement et analytiquement dans le cas unidimensionnel. À l'EP, on constate une très forte atténuation quand l'excitation correspond exactement aux modes fusionnés. En revanche, l'excitation du vecteur propre généralisé peut limiter cet effet.

1 Introduction

The design of acoustic treatments for sound attenuation in acoustics waveguides such as ventilation systems, exhaust devices, and aircraft engines is still a challenge for transportation and building industries. Recent studies showed how to maximize the axial wavenumber attenuation with locally reacting liners [17, 1] porous [13] and metaporous liners [20] by tuning the parameters of the system on an exceptional point (EP).

An EP is a special property of non-Hermitian systems where the operator/matrix becomes defective, meaning that two (possibly more) eigenvalues coalesce as well as their associated eigenvectors. In this context, EP correspond to double roots in the dispersion equation.

EP attracted a lot of attention in the last decade in various domain of physics, especially quantum mechanics and photonics [8] (see references therein), but the concept of mode merging design is nothing new. Actually, one one the most used method for the design of acoustics liner, the Cremer's impedance, developed by Cremer [3] and then improved by Tester [17, 18], and which refers to the optimal impedance that will maximize the attenuation of an individual mode in a uniform waveguide corresponds to an EP. However, where the Cremer's impedance only refers to locally reacting boundary condition, the EP based design generalizes this concept to non-locally reacting materials [20, 13].

At stated previously, such EP occurs generically in non-Hermitian system, that is, a system with gain or loss, where the modes are not orthogonal anymore. This properties is increased near an EP. Therefore the modes themselves are not sufficient enough to give a complete description of the system, but their interactions have to be taken into account too [19, 1, 6].

Concerning finite size systems, the eigenvalues represent the eigenfrequencies and their imaginary part is the exponential decay rate. Some preliminary studies were performed on two degrees-of-freedom (2DOF) coupled oscillators [16, 14, 4] show that EP yields to the best time decay for both oscillators. It appears that EP defines a limit between strong and weak coupling [14], explaining its importance in the energy transfer (beat) between the host and the acoustic treatment. The concept of defective eigenvalue also appears in some tuning strategies for tuned mass damper (TMD) [7] which leads to a different damping ratio from the well known defined by Den Hartog. However this strategy doesn't provide the best decay rate [2].

The present study aims to generalize this concept to a continuous system and to adapt some generic methods to locate EP [10, 5] to find real parameters. In addition, the influence of the incomplete modal basis and the generalized eigenvector, especially in transient regime, is also investigated.

First, the section 2 defines the problem and presents the dispersion equation in order to find the EP. The section 3 introduces the time domain finite element model to solve the wave propagation. Finally, the section 4 show the results on the reverberation time.

2 Problem statement

2.1 Physical model

We consider a one-dimensional cavity of length L and section S filled with air of density ρ_0 and sound speed c_0. This cavity is coupled with a single degree-of-freedom (SDOF) resonator modeled by a damped spring-mass system of mass m_r, stiffness k_r and damping c_r.

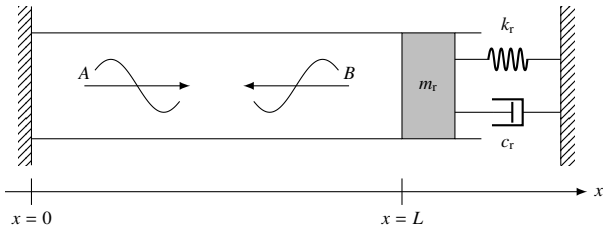

FIGURE 1 – Sketch of the one-dimensional acoustic cavity coupled with a damped spring-mass system.

The wave propagation inside the cavity is governed by the wave equation

$$\nabla^2\Phi - \frac{1}{c_0^2}\frac{\partial^2\Phi}{\partial t^2} = 0, \tag{1}$$

where Φ is the velocity potential, from which we can recover

both the particle velocity

$$\mathbf{v} = \nabla\Phi, \tag{2}$$

and the sound pressure

$$p = -\rho_0 \frac{\partial \Phi}{\partial t}. \tag{3}$$

The equation of motion of the SDOF resonator reads

$$m_\mathrm{r}\ddot{u} + c_\mathrm{r}\dot{u} + ku_\mathrm{r} = F, \tag{4}$$

where u is displacement from equilibrium and F the external force acting on the resonator.

We consider here only time harmonic perturbation ($\mathrm{e}^{-\mathrm{i}\omega t}$ convention). With the rigid wall condition at $x = 0$, the velocity potential in the cavity is given by

$$\Phi(x,t) = \phi\cos(kx)\mathrm{e}^{-\mathrm{i}\omega t}, \tag{5}$$

where ϕ is the amplitude and k and ω are the wavenumber and angular frequency respectively. Both quantities are related by $\omega = kc_0$. The harmonic motion of the resonator is

$$u(t) = u_0\mathrm{e}^{-\mathrm{i}\omega t}. \tag{6}$$

The coupling conditions $\mathbf{v}(x = L)\cdot\mathbf{n} = \dot{u}$ and $F = pS$ yield the system of equations

$$\begin{bmatrix} k\sin(kL) & -\mathrm{i}\omega \\ -\mathrm{i}\rho_0 S\,\omega\cos(kL) & -m_\mathrm{r}\omega^2 - \mathrm{i}c_\mathrm{r}\omega + k_\mathrm{r} \end{bmatrix}\begin{bmatrix} \phi \\ u_0 \end{bmatrix} = \begin{bmatrix} 0 \\ 0 \end{bmatrix}, \tag{7}$$

which is a nonlinear eigenvalue problem. The angular eigenfrequencies of the system are the roots of the determinant, that is, if we write everything as a function of ω

$$f(\omega) = \frac{\omega}{c_0}\left(-m_\mathrm{r}\omega^2 - \mathrm{i}c_\mathrm{r}\omega + k_\mathrm{r}\right)\sin\left(\frac{\omega L}{c_0}\right) + \rho_0 S\,\omega^2\cos\left(\frac{\omega L}{c_0}\right). \tag{8}$$

This equation can be solved with contour integral solver like [12, 9] based on the argument principle.

Since at the EP, an angular eigenfrequency ω_0 must be a double root of f, it means that ω_0 is a root of both f and $\partial_\omega f$. To enforce this condition we can either use one complex valued or two real valued parameters.

2.2 Numerical continuation

Finding EP and imposing real parameter is not trivial. We use here a two steps method. First, $f(\omega, c_\mathrm{r}; k_\mathrm{r}) = 0$ and $\partial_\omega f(\omega, c_\mathrm{r}; k_\mathrm{r}) = 0$ can be combined into one scalar equation involving the unknown parameter c_r assuming k_r is known. As before, this equation can be solved with contour integral solver.

For an arbitrary value of k_r, this yields to *complex* value of c_r. Since there is a continuum of EP if we can add a parameter (here k_r) and used a continuation method based on ODE solving to find the value of k_EP that leads to *real valued* c_EP. To do so, it is convenient to introduce the EP system

$$\mathbf{F}(\omega, c_\mathrm{r}; k_\mathrm{r}) = \begin{bmatrix} f(\omega, c_\mathrm{r}; k_\mathrm{r}) \\ \partial_\omega f(\omega, c_\mathrm{r}; k_\mathrm{r}) \end{bmatrix}. \tag{9}$$

We start from the the initial solution obtained at the first step and track the solution path until c_EP is real.

3 Time domain numerical modeling

3.1 Numerical solution of the wave equation

The wave equation is a second-order linear partial differential equation (PDE) which depends on x and t. In order to solve it numerically we discretize the solutions domains in both space and time using the finite element method (FEM) and Newmark-beta method respectively.

The weak formulation associated with the wave equation Eq. (1) gives

$$\int_0^L \frac{1}{c_0^2}\Psi(x)\frac{\partial^2\Phi(x,t)}{\partial t^2}\,\mathrm{d}x + \int_0^L \frac{\partial\Psi}{\partial x}(x)\frac{\partial\Phi(x,t)}{\partial x}\,\mathrm{d}x = \Psi(L)\frac{\partial\Phi(L,t)}{\partial x}, \tag{10}$$

where Ψ stands for the test function. Once the weak formulation is discretized with the Lagrange finite element, we get the matrix form

$$\mathbf{M}\ddot{\mathbf{\Phi}} + \mathbf{K}\mathbf{\Phi} = \begin{bmatrix} \mathbf{0} \\ \frac{\partial\Phi_n(t)}{\partial x} \end{bmatrix}. \tag{11}$$

Here, the vector $\mathbf{\Phi}$ contains the instantaneous finite element nodal values of the velocity potential

$$\mathbf{\Phi} = \begin{bmatrix} \Phi_1(t) & \Phi_2(t) & \cdots & \Phi_n(t) \end{bmatrix}^\mathrm{T}, \tag{12}$$

and $\mathbf{M}$ and $\mathbf{K}$ are the standard mass and stiffness matrices respectively. Combining equations (4) and (11) with the coupling conditions we get the augmented second-order (in time) system of linear equations

$$\begin{cases} \mathbf{M}\ddot{\mathbf{\Phi}} + \mathbf{K}\mathbf{\Phi} = \begin{bmatrix} \mathbf{0} \\ \dot{u} \end{bmatrix}, \\ m_\mathrm{r}\ddot{u} + c_\mathrm{r}\dot{u} + k_\mathrm{r}u = -\rho_0 S\,\dot{\Phi}_n, \end{cases} \tag{13}$$

which can be written in matrix form

$$\begin{bmatrix} \mathbf{M} & \mathbf{0} \\ \mathbf{0} & m_\mathrm{r} \end{bmatrix}\begin{bmatrix} \ddot{\mathbf{\Phi}} \\ \ddot{u} \end{bmatrix} + \begin{bmatrix} \mathbf{0} & \mathbf{C_1} \\ \mathbf{C_2} & c_\mathrm{r} \end{bmatrix}\begin{bmatrix} \dot{\mathbf{\Phi}} \\ \dot{u} \end{bmatrix} + \begin{bmatrix} \mathbf{K} & \mathbf{0} \\ \mathbf{0} & k_\mathrm{r} \end{bmatrix}\begin{bmatrix} \mathbf{\Phi} \\ u \end{bmatrix} = \mathbf{0}, \tag{14}$$

with coupling coefficient matrix

$$\mathbf{C_1} = \begin{bmatrix} \mathbf{0} \\ -1 \end{bmatrix} \tag{15}$$

and

$$\mathbf{C_2} = \begin{bmatrix} \mathbf{0} & \rho_0 S \end{bmatrix}. \tag{16}$$

After applying the initial condition, this second order differential equation is solved numerically using the Newmark-beta method [11] applied with average constant acceleration method ($\gamma = 1/2$ and $\beta = 1/4$) which is unconditionally stable.

3.2 Sound energy

We will use the energy to help quantifying the attenuation or our system. Thus we need to compute it in both the cavity and the resonator.

The mechanical energy E_r of the resonator is given by

$$E_\mathrm{r} = \frac{1}{2}k_\mathrm{r}u^2 + \frac{1}{2}m_\mathrm{r}\dot{u}^2. \tag{17}$$

The sound energy density w in the cavity, obtained from the continuity equation, Euler equation and equation of state, is given by

$$w = \frac{1}{2}\frac{p^2}{\rho_0 c_0^2} + \frac{1}{2}\rho_0 v^2, \tag{18}$$

which once integrated over the cavity volume gives the sound energy W

$$W = \int_V \frac{1}{2}\frac{p^2}{\rho_0 c_0^2}\,\mathrm{d}V + \int_V \frac{1}{2}\rho_0 v^2\,\mathrm{d}V. \tag{19}$$

Once again working with the velocity potential Φ allows us to simplify the calculus and we get

$$W = \frac{1}{2}\rho_0 S\int_0^L \frac{1}{c_0^2}\frac{\partial\Phi}{\partial t}\frac{\partial\Phi}{\partial t}\,\mathrm{d}x + \frac{1}{2}\rho_0 S\int_0^L \frac{\partial\Phi}{\partial x}\frac{\partial\Phi}{\partial x}\,\mathrm{d}x, \tag{20}$$

which can be expressed with the mass and stiffness matrices

$$W = \frac{1}{2}\rho_0 S\,\dot{\mathbf{\Phi}}^\mathrm{T}\mathbf{M}\dot{\mathbf{\Phi}} + \frac{1}{2}\rho_0 S\,\mathbf{\Phi}^\mathrm{T}\mathbf{K}\mathbf{\Phi}. \tag{21}$$

It is noteworthy that $\dot{\mathbf{\Phi}}$ is also computed at each time step by the integration scheme. We note $E = E_\mathrm{r} + W$, the total energy.

The numerical model has been validated by comparing the variation of the total energy $\frac{\mathrm{d}E}{\mathrm{d}t}$ and the power loss $-c_\mathrm{r}\dot{u}^2$. These 2 are identical up to the discretization error.

4 Results

4.1 Modal attenuation

We fix $L = S = \rho_0 = 1$ and $m_\mathrm{r} = 1$ so the mass of air in the cavity is equal to the mass of the resonator. By fixing the speed of sound $c_0 = 1$, we found an EP for the first two modes (sorted by $\mathrm{Re}\,\omega$) for $k_\mathrm{r} = 10.313$ and $c_\mathrm{r} = 3.0620$ with an angular frequency of $\omega = 3.0797 - \mathrm{i}0.6570$. In order to understand how the EP is linked to an optimal damping, we plot in Figure 2 the complex angular frequencies of the two modes concerned by this EP as a function of the damping c_r with $k_\mathrm{r} = k_\mathrm{EP}$.

Here the imaginary part of ω refers to the exponential decay rate of the mode, that is $\lambda = -\mathrm{Im}\,\omega$. We can distinguish two regimes :

- when $c_\mathrm{r} \ll c_\mathrm{EP}$ both modes share close decay constant, which is increased by increasing the damping ;
- when $c_\mathrm{r} \gg c_\mathrm{EP}$ increasing the damping increase the decay constant of one mode but decrease the one of the other mode.

The least attenuated mode will dominate the transient state, thus choosing $c_\mathrm{r} \simeq c_\mathrm{EP}$ is an efficient design method as it leads to a great attenuation for the least attenuated mode.

Figure 3 presents the decay rate of the least attenuated mode for different values of k_r and c_r. As expected, the set

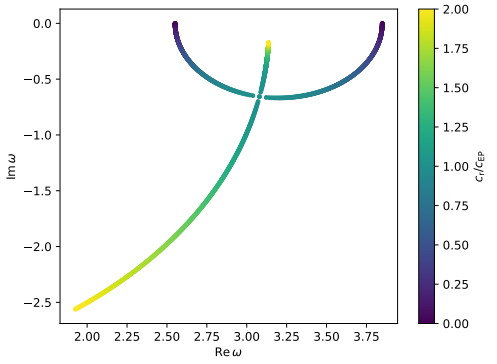

FIGURE 2 – Evolution of the two first angular frequencies of the coupled system as a function of c_r with $k_\mathrm{r} = k_\mathrm{EP}$.

of parameters that ensure the least attenuated mode to be the more attenuated is close to the EP. This modal decay rate is supposed to be valid at long time. The next section will investigate the transient behavior of the system.

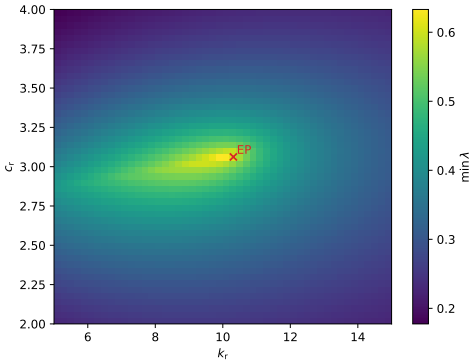

FIGURE 3 – Least attenuated decay rate of the two first angular frequencies of the coupled system as a function of c_r and k_r.

4.2 Energy

As stated previously, because of the loss of orthogonality the modes themselves are not sufficient enough to give a complete description of the system, but their interactions have to be taken into account too. In order to illustrate this, we will study the total energy of the system during the transient state for different initial conditions. Because our EP concerns only the first two modes, their eigenvectors will be chosen as initial conditions in the vicinity of the EP,

$$\mathbf{v}_n(x) = \begin{cases} \Phi(x) = \phi_n \cos\left(\frac{\omega_n x}{c_0}\right), \\ u = -\mathrm{i}\frac{\phi_n}{c_0}\sin\left(\frac{\omega_n L}{c_0}\right), \end{cases} \tag{22}$$

where the amplitude ϕ_n is chosen such that each mode has a initial energy of 1.

First, the initial conditions are chosen as the sum of the eigenvectors to excite only the true eigenvector. In Figure 4a

$c_r/c_{EP} = 0.8$, $\omega_1 = 2.7306 - i0.4626$ and $\omega_2 = 3.5219 - i0.5800$. In Figure 4c $c_r/c_{EP} = 1$ and $\omega_0 = 3.0797 - 0.6570i$. As we are at the EP, there is only one mode, therefore the energy decreases as $e^{-2\lambda_{EP}t}$ (red dotted line) as predicted by Eq. (20). In Figure 4e $c_r/c_{EP} = 1.2$, $\omega_1 = 3.1241 - i0.3511$ and $\omega_2 = 2.9118 - i1.2392$. The second mode is way more attenuated than the first one and vanished quickly, hence the first mode dominated the system response at long term.

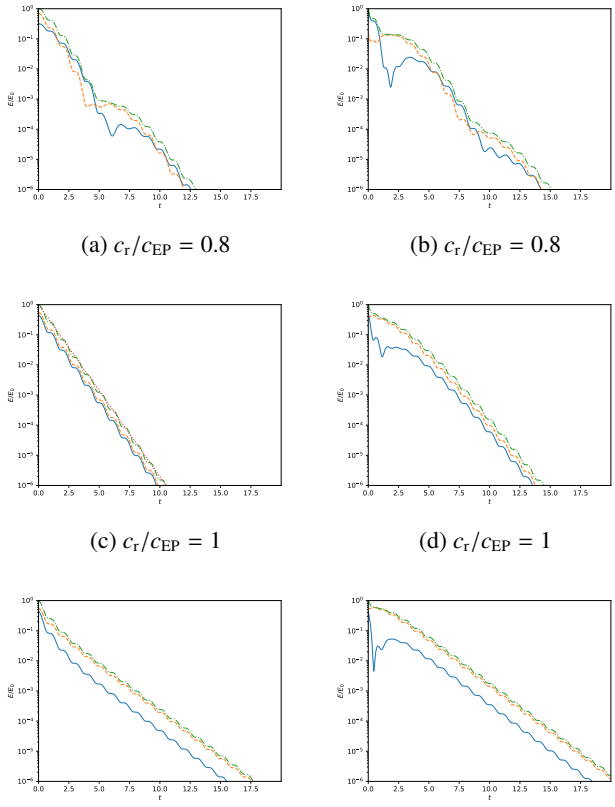

(a) $c_r/c_{EP} = 0.8$ (b) $c_r/c_{EP} = 0.8$

(c) $c_r/c_{EP} = 1$ (d) $c_r/c_{EP} = 1$

(e) $c_r/c_{EP} = 1.2$ (f) $c_r/c_{EP} = 1.2$

FIGURE 4 – (color online) Evolution of the SDOF mechanical energy (blue solid line), cavity energy (orange dashed line) and total energy (green dash-dotted line) with respect to the distance to c_{EP}. In (c) the red dotted line corresponds to $e^{-2\lambda_{EP}t}$ The energy is normalized and plot in log scale. In (a, c, e) the sum of the first two mode shapes are imposed as initial condition. In (b, d, f) the difference is imposed. In all cases $m_r = 1$, $k_r = k_{EP}$.

It is interesting to compare those results to the notion of weak and strong coupling in the case of coupled oscillators. The first refers to the exchange of energy between the two oscillators (beat) happening when the coupling dominates the loss, while the latter corresponds to the case where both oscillators saw their energy decrease through time. It was discussed that the transition between those two states was explained by the presence of an EP [14, 4].

Then, the initial condition are chosen as the difference of the eigenvectors to excite also the generalized eigenvector. In this case the energy exhibits a significantly different behavior especially at early time. This is due to an additional time growing contribution that may be explained by the the beat of two modes with almost the same frequency. Indeed, at the EP, not only the two eigenvectors will coalesce, but a generalized eigenvector will be generated. Unlike an eigenvector, a generalized eigenvector alone is not a solution of Eq. (7). If we note $\mathbf{v}_0(x)$ the eigenvector from Eq. (22) and $\mathbf{v}_1(x)$ its associated generalized eigenvector then $\mathbf{v}_0(x)e^{-i\omega_0 t}$ and $(\mathbf{v}_1(x) - it\mathbf{v}_0(x))e^{-i\omega_0 t}$ are solutions of the problem when it is tuned on the EP. The latter, which involves the $te^{-i\omega_0 t}$, may explained the results obtained in Figure 4 as its related to the difference of the two merging modes in the vicinity of the EP.

5 Conclusion

In this study, it has been shown that tuning the system on an EP is an efficient design method for low frequency noise control. This approach is very general and ensure a great decay rate for the targeted modes. Especially, due to the high loss of orthogonality of these modes in the EP vicinity, the best reverberation time is obtained when the excitation is close to the eigenvector. We also demonstrate that is was possible to obtain EP with real parameters, allowing us to perform study in the transient regime and making this solution manufacturable. Further investigations need to be done to inspect the impact of the generalized eigenvector on the system as well as to compare this method with other design strategies like those based on perfect absorption [15].

Références

[1] W. Bi et V. Pagneux. « New insights into mode behaviours in waveguides with impedance boundary conditions ». In : *arXiv :1511.05508 [quant-ph]* (2015).

[2] P. Bisegna et G. Caruso. « Closed-form formulas for the optimal pole-based design of tuned mass dampers ». In : *Journal of Sound and Vibration* 331.10 (2012), p. 2291-2314.

[3] L. Cremer. « Theory regarding the attenuation of sound transmitted by air in a rectangular duct with an absorbing wall, and the maximum attenuation constant produced during this process ». In : *Acustica* 3.1 (1953), p. 249-263.

[4] G. Dolfo et J. Vigué. « Damping of coupled harmonic oscillators ». In : *European Journal of Physics* 39.2 (2018), p. 025005.

[5] M. Ghienne et B. Nennig. « Beyond the limitations of perturbation methods for real random eigenvalue problems using Exceptional Points and analytic continuation ». In : *Journal of Sound and Vibration* 480 (2020), p. 115398.

[6] W. Guo et al. « Spatial transient behavior in waveguides with lossy impedance boundary conditions ». In : *arXiv :2010.03646 [physics]* (2020).

[7] S. Krenk. « Frequency Analysis of the Tuned Mass Damper ». In : *Journal of Applied Mechanics* 72.6 (2005), p. 936-942.

[8] M.-A. Miri et A. Alù. « Exceptional points in optics and photonics ». In : *Science* 363.6422 (2019), eaar7709.

[9] B. Nennig. *polze : A python package to locate poles and zeros of a meromorphic function with their multiplicities*. 2021.

[10] B. Nennig et E. Perrey-Debain. « A high order continuation method to locate exceptional points and to compute Puiseux series with applications to acoustic waveguides ». In : *Journal of Computational Physics* 412 (2020), p. 109425.

[11] N. M. Newmark. « A Method of Computation for Structural Dynamics ». In : *Journal of the Engineering Mechanics Division* 85.3 (1959), p. 67-94.

[12] R. Parini. *cxroots : A Python module to find all the roots of a complex analytic function within a given contour*. 2022.

[13] X. Qiu et al. « Optimality analysis of bulk-reacting liners based on mode-merging design method ». In : *Journal of Sound and Vibration* 485 (2020), p. 115581.

[14] S. R.-K. Rodriguez. « Classical and quantum distinctions between weak and strong coupling ». In : *European Journal of Physics* 37.2 (2016), p. 025802.

[15] V. Romero-García et al. « Perfect and broadband acoustic absorption by critically coupled sub-wavelength resonators ». In : *Scientific Reports* 6.1 (2016), p. 19519.

[16] J.-W. Ryu et al. « Exceptional points in coupled dissipative dynamical systems ». In : *Physical Review E* 91.5 (2015), p. 052910.

[17] B. J. Tester. « The optimization of modal sound attenuation in ducts, in the absence of mean flow ». In : *Journal of Sound and Vibration* 27.4 (1973), p. 477-513.

[18] B. J. Tester. « The propagation and attenuation of sound in lined ducts containing uniform or "plug" flow ». In : *Journal of Sound and Vibration* 28.2 (1973), p. 151-203.

[19] L. N. Trefethen et M. Embree. *Spectra and Pseudospectra : The Behavior of Nonnormal Matrices and Operators*. Princeton University Press, 2005.

[20] L. Xiong et al. « Sound attenuation optimization using metaporous materials tuned on exceptional points ». In : *The Journal of the Acoustical Society of America* 142.4 (2017), p. 2288-2297.